

Superfluid density of high- T_c cuprate systems: implication on condensation mechanisms, heterogeneity and phase diagram

Y.J. Uemura *

Department of Physics, Columbia University, New York, NY 10027, USA

Extensive muon spin relaxation (μ SR) measurements have been performed to determine the magnetic field penetration depth λ in high T_c cuprate superconductors with simple hole doping, Zn-doping, overdoping, and formation of static SDW nano islands. System dependence of n_s/m^* (superconducting carrier density / effective mass) reveals universal correlations between T_c and n_s/m^* in all these cases with/without perturbation. Evidence for spontaneous and microscopic phase separation into normal and superconducting regions was obtained in the cases with strong perturbation, i.e., Zn-doping (swiss cheese model), overdoping, and coexisting magnetic and superconducting states (SDW nano islands). The length scale of this heterogeneity is shown to be comparable to the in-plane coherence length. We discuss implication of these results on condensation mechanisms of HTSC systems, resorting to an analogy with pure ^4He and $^4\text{He}/^3\text{He}$ mixture films on regular and porous media, reminding essential features of Bose-Einstein, BCS and Kosterlitz-Thouless condensation/transition in 3-d and 2-d systems, and comparing models of BE-BCS crossover and phase fluctuations. Combining the μ SR results on n_s/m^* and the pseudo-gap behavior, we propose a new phase diagram for HTSC, characterized by: (1) the T^* line that represents pair formation; (2) disappearance of this line above the critical hole concentration $x = x_c$; (3) in the underdoped region between T_c and T^* , there exists another line T_{dyn} which corresponds to the onset of dynamic superconductivity with superconducting phase fluctuations; and (4) the overdoped region being phase separated between hole-poor superfluid and hole-rich normal fermion metal regions. Finally, we elucidate anomalous reduction of superfluid spectral weight in the crossover from superconducting to metallic ground states found not only in overdoped HTSC cuprates but also in pressurized organic BEDT and A_3C_{60} fulleride superconductors.

I. INTRODUCTION

Muon spin relaxation (μ SR) technique [1-3] has made significant contributions to studies of high- T_c superconductors (HTSC). Measurements in transverse-fields (TF- μ SR) provide a reliable way to determine the magnetic field penetration depth λ of type-II superconductors and to infer details of the flux vortex lattice, while measurements in zero-field (ZF- μ SR) allow studies of static magnetism, leading to determination of the phase diagrams, local spin structures, and volume fraction of static magnetism. In this article, we provide a perspective view on

development of these measurements in HTSC systems and their implications on condensation mechanisms, heterogeneity and phase diagrams, focusing on the behavior of n_s/m^* (superconducting carrier density / effective mass). Since the parameter n_s/m^* in HTSC systems plays a role similar to the superfluid density in superfluid He systems, we refer to it as “superfluid density” in the title and the text of this paper.

In the following section, Section II, we start with the results of the penetration depth measurements of hole-doped cuprate systems, which exhibit universal correlations between T_c and n_s/m^* . We discuss these correlations in terms of energy scales of superconducting carriers. Then, we look into the cases involving heterogeneity, i.e., (Cu,Zn) substitution and overdoping in Section III, and systems with coexisting superconductivity and static magnetism, with the formation of magnetic nano-islands, in section IV. In all these cases, the superfluid density has a trade-off with the volume of non-superconducting regions created by perturbation and/or phase separation. We shall see that the universal correlations between T_c and the superfluid density n_s/m^* are followed not only by the simple hole doped cuprates but also by these HTSC systems with microscopic phase separation.

Thin films of superfluid ^4He and $^4\text{He}/^3\text{He}$ mixtures represent another set of systems where the superfluid transition temperature T_c is strongly correlated with the superfluid density. In section V, we compare the results of HTSC systems with superfluid He films in normal and porous media.

Based on the correlations between T_c and n_s/m^* and the pseudogap phenomena in the underdoped region, some models/conjectures have been presented in terms of the condensation mechanisms of HTSC systems. To elucidate these models, in section VI, we will first consider differences and similarities among Bose-Einstein (BE) condensation, BCS condensation and Kosterlitz-Thouless (KT) transition. Then, we will compare models of BE-BCS crossover and phase fluctuations, taking into account relevance to the KT transition and distinction between pair-formation and dynamic superconductivity in the pseudo-gap regime. We will also introduce a phase diagram involving phase separation in the overdoped region in section VII, followed by a summary in section VIII.

II. CORRELATIONS BETWEEN T_c AND N_S/M^* IN HOLE-DOPED HTSC

In type-II superconductors, the external magnetic field, between H_{c1} and H_{c2} , forms a lattice of flux vortices, resulting in inhomogeneous internal field distributions. The width of this distribution is proportional to the muon spin relaxation rate σ in TF- μ SR, which is related to the penetration depth λ and n_s/m^* as

$$\sigma \propto \lambda^{-2} = [4\pi n_s e^2 / c^2] \times [1 / (1 + \xi / l)] \quad (1),$$

as given by the London equation. In superconducting systems in the clean limit, where the coherence length ξ is much shorter than the mean free path l , the relaxation rate σ is proportional to n_s/m^* . The inhomogeneity of the internal field is due to partial screening of the external field by the supercurrent. So, it is quite natural that the field width and σ are proportional to the ‘‘supercurrent density’’ n_s/m^* , in the same sense as the conductivity of normal metals is proportional to n_n/m^* , where n_n denotes the normal state carrier density.

Generally, TF- μ SR studies in type-II superconductors provide information on: (a) the temperature dependence of λ ; (b) absolute values of λ at $T \rightarrow 0$; (c) the coherence length ξ via analyses of local field distribution; and (d) vortex lattice properties. Among these, use of single crystal specimens is essential in (a), (c) and (d). For example, early μ SR results of λ on ceramic samples of HTSC systems mostly exhibited behavior consistent with isotropic energy gap, and it is only after studies of high-quality single crystal specimens that the d-wave nature was confirmed in temperature dependence of λ . For details of (a), (c) and (d), readers are referred to refs. [3-4].

In contrast, the results on ceramic specimens have been very useful in comparing absolute values of n_s/m^* in different systems. Ceramic specimens provide advantages over single crystal specimens in homogeneity of doped hole concentrations and in being less affected by crossover from the 3-d to 2-d vortex lattice. In this article, we shall focus on the system and doping dependence of the superfluid density, i.e., (b). In HTSC systems with a large anisotropy, the relaxation rate σ measured in ceramic specimens is determined predominantly by the supercurrent flowing in the conducting ab-planes [5]. Thus, the results of σ from ceramic specimens should be regarded as reflecting the in-plane penetration depth λ_{ab} and the in-plane effective mass m_{ab}^* .

Figure 1 shows a plot of $\sigma(T \rightarrow 0)$ versus T_c of various different HTSC systems [6-11]. In this figure, results from simple hole-doped HTSC systems [6,7] are shown with open symbols. With increasing hole concentration, T_c increases linearly with n_s/m^* in the underdoped region, and then shows a saturation. The slope of this linear relationship in the underdoped region is common to various different series of HTSC systems. These results have also been confirmed in several other μ SR measurements [12-16]. This observation alone already implies that n_s/m^*

can be an important determining factor for T_c in HTSC systems. We also find in Fig. 1 that the ratios of T_c versus n_s/m^* for some other superconductors [17,18] are not quite far from the value for HTSC systems.

If an independent estimate for the effective mass m^* is available, the μ SR measurements give the superconducting carrier density n_s . Then, one can calculate the number of carries existing in a region of coherence length squared on the conducting plane. For typical BCS superconductors, such as Sn or Pb, one finds more than 10,000 pairs overlapping with one another in the $\pi\xi^2$ area. For superfluid He, which is the well-known case for Bose-Einstein condensation, we find that each boson exist without overlapping with each other: i.e., one pair per $\pi\xi^2$. The systems following the linear relationship in Fig. 1 have 3 to 6 pairs overlapping within the $\pi\xi^2$ area, as illustrated in Fig. 2. This feature encourages us to consider HTSC and some novel superconductors in a crossover from BE to BCS condensation.

By knowing the average distance c_{int} between the conducting CuO_2 planes, one can obtain n_{s2d}/m^* where n_{s2d} denotes the 2-dimensional carrier density. We remind here that the Fermi energy ϵ_F of 2-dimensional electron gas is proportional to n_{n2d}/m^* . Thus, we can consider n_{s2d}/m^* as a parameter representing kinetic energy for translational motion of superconducting carries. For 3-d systems without phase separation, in which $n_n = n_s$, one can combine the muon relaxation rate $\sigma \propto n_s/m^*$ with the Sommerfeld constant $\gamma(T = T_c) \propto n_n^{1/3} m^*$, or Pauli susceptibility $\chi(T = T_c) \propto n_n^{1/3} m^*$, to deduce $\epsilon_F \propto n_s^{2/3}/m^*$. The ‘‘effective’’ Fermi energy ϵ_F obtained in this way does not necessarily correspond to the real Fermi energy in band structure calculations. Since $1/\lambda^2$ corresponds to the Drude spectral weight in optical conductivity which condenses into a delta function at $\omega = 0$ below T_c , ϵ_F might also be called as a Drude energy scale.

Figure 3 shows a plot of T_c versus $T_F = \epsilon_F/k_B$ thus obtained from the results of n_s/m^* [7]. For A_3C_{60} where a reliable value of l is not available, we used the clean-limit value of n_s/m^* without corrections regarding ξ/l [17,18]. We find that HTSC, organic BEDT [19], and some other systems [17-20] have very high and nearly equal ratios of T_c/T_F . The T_B line in this figure shows the Bose-Einstein condensation temperature for a non-interacting 3-d Bose gas having the boson density $n_B = n_s/2$ and mass $m_B = 2m^*$. Compared to T_B , the actual transition temperatures T_c of HTSC systems are reduced by a factor of 4 to 5. This reduction is natural in view of overlapping pairs which would reduce T_c , and in view of 2-dimensional character of HTSC systems. However the parallel behavior of T_B and the observed results of T_c suggests that the origin of the linear relationship between T_c and n_s/m^* could be deeply related to BE condensation. Figure 3 serves as an empirical way to classify various superconductors in a crossover from BE to BCS condensation.

III. HTSC SYSTEMS INVOLVING MICROSCOPIC HETEROGENEITY: ZN-DOPING AND OVERDOPING

A. (Cu,Zn) substitution

When a very small amount of Zn is substituted for Cu on the CuO_2 planes of HTSC systems, T_c is reduced. Figure 4(a) shows the reduction of $\sigma(T \rightarrow 0)$ as a function of Zn concentration c substituting in-plane Cu. The superfluid density n_s/m^* decreases with increasing c . To account for this reduction, we proposed ‘‘Swiss Cheese Model’’ [9] where each Zn is assumed to destroy superconductivity in the surrounding region with the area $\pi\xi_{ab}^2$, as illustrated in Fig. 4(a). The solid lines in Fig. 4(a), which represent predictions of this model, are obtained just from c and ξ_{ab} deduced from the upper critical field H_{c2} , *without any fitting* to the data. Sufficiently good agreement between these lines and the observed results indicate that carriers within the $\pi\xi_{ab}^2$ area around each Zn no longer contribute to the superfluid density n_s/m^* . Subsequently, this picture was directly confirmed by Pan *et al.* [21] in Scanning Tunneling Microscopy studies, where the local density of states around Zn showed features characteristic to normal regions, as shown in Fig. 4(b). These μSR and STM results are consistent with the non-zero γ term of the specific heat, which increases with increasing Zn concentration [22]. In the plot of σ versus T_c in Fig. 1, the results of Zn-doped systems (closed triangle and star symbols) follow the trajectory of simple hole doped HTSC systems (open symbols).

B. overdoping

$\text{Tl}_2\text{Ba}_2\text{CuO}_{6+\delta}$ (Tl2201) systems have been extensively studied by various experimental methods as a prototype of overdoped HTSC systems. Tl2201 compounds have very small residual resistivity, which assures that the system lies well within the clean limit. To our surprise, with increasing overdoping from the nearly optimal $T_c = 85$ K sample, the relaxation rate $\sigma(T \rightarrow 0)$ in TF- μSR decreased [8,15] as shown by the closed circle symbols in Fig. 1. This behavior is also shown in a plot of $\sigma(T \rightarrow 0)$ versus doping factor δ in Fig. 5(a). In view of no anomaly in m^* , the different behaviors of the normal state carriers n_n and the superfluid density n_s/m^* suggest that carriers are spontaneously separated into those which are involved in superconductivity and those which remain unpaired fermions, as illustrated in Fig. 5(a).

By defining the ‘‘gapped’’ and ‘‘ungapped’’ responses in the specific heat measurements, as illustrated in Fig. 5(a), we plotted the δ dependence of the gapped response obtained from the data of Loram *et al.* [22] in Tl2201 in Fig. 5(a). The good agreement between the μSR superfluid density $\sigma(T \rightarrow 0)$ (closed circles) and the ‘‘gapped’’

response in specific heat (open symbols) provides a support to our view [8,23] with spontaneous phase separation between superconducting and normal regions in overdoped HTSC systems.

The volume fraction of the superconducting region can also be estimated from the ‘‘specific heat jump’’ ΔC . In BCS superconductors $\Delta C \propto C_n \propto \gamma_n T$, where C_n denotes the normal-state specific heat, and γ_n stands for the Sommerfeld constant derived in the normal state. Then, in the plot of C/T versus T as in the inset of Fig. 5(a), one would expect that the specific heat jump $\Delta C/T$ should be independent of T_c , for systems having a common γ_n value. In Loram’s specific heat results of Tl2201 [22], γ_n does not depend on doping, while the jump $\Delta C/T$ decreases with increasing doping. This observation further supports decreasing superfluid volume fraction with increasing doping (decreasing T_c) in Tl2201.

Residual normal response in the overdoped cuprate was also found in measurements of optical conductivity [24]. Furthermore, we calculated an expected doping dependence of n_s/m^* based on a simple model assuming phase separation [23] (as described in section VII), and obtained a good agreement with the observed results in $(\text{Y,Ca})\text{Ba}_2\text{Cu}_3\text{O}_y$ [25], as shown in Fig. 5(b). So far, there is no direct observation reported regarding the size of these phase-separated regions in overdoped HTSC.

IV. HTSC SYSTEMS WITH STATIC SDW NANO-ISLANDS

Magnetic order of the parent compound La_2CuO_4 of the 214 cuprates was first confirmed by ZF- μSR measurements [26]. Figure 6(a) shows the time spectra obtained in the ZF measurements of antiferromagnetic La_2CuO_4 (AF-LCO) which has the Néel temperature $T_N > 250$ K. As in most other magnetic systems, we find that muon spin precession sets in below T_N , with the precession amplitude independent of temperature, while the frequency increasing with decreasing temperature as the sub-lattice magnetization builds up. In the La214 systems with the hole concentration near 1/8 per Cu, incommensurate static spin correlations have been found by neutron scattering [27]. Time spectrum of ZF- μSR in $\text{La}_{1.875}\text{Ba}_{0.125}\text{CuO}_4$ (LBCO:0.125) [28] is shown in Fig. 6(b). In this case, we find a Bessel function line shape characteristic of ZF- μSR in incommensurate magnetic systems [29,30], such as the one observed in $(\text{TMTSF})_2\text{PF}_6$ [29].

$\text{La}_2\text{CuO}_{4.11}$ (LCO:4.11) is a system with oxygen intercalated in a stage-4 structure. This system is superconducting with $T_c = 42$ K, which is the highest among the La214 family, while also exhibiting static incommensurate magnetism below $T_N = 42$ K [31] This incommensurate modulation has a very long correlation length (≥ 600 Å), as determined from a very sharp satellite magnetic Bragg peak in neutron scattering results. ZF- μSR

spectra of this system [10,32], shown in Fig. 6(c), has a Bessel-function line shape, as expected for an incommensurate spin structure. The amplitude of this precession, however, increases gradually below T_N with decreasing temperature, while the frequency is almost independent of temperature below T_N . Furthermore, the amplitude of precessing signal at $T \rightarrow 0$ is less than half of that in LBCO:0.125 (Fig. 6(b)), which indicates that the static magnetism exists in less than a half of the total volume.

In Fig. 7(a) and (b), we show temperature dependences of the volume fraction V_M of muons in the region with static magnetic freezing, derived from the precession amplitude, and the frequency ν observed in LCO:4.11, $(\text{La}_{1.88}\text{Sr}_{0.12})\text{CuO}_4$ (LSCO:0.12), LBCO:0.125 and $(\text{La}_{1.475}\text{Nd}_{0.4}\text{Sr}_{0.125})\text{CuO}_4$ (LNSCO:0.125) [33]. In LCO:4.11 and LSCO:0.12, where superconductivity coexists with static magnetism, the static magnetism is confined to a partial volume fraction. As shown in Fig. 7(c), the temperature dependence of the neutron Bragg intensity in LCO:4.11 is consistent with the behavior of $V_M\nu^2$. Unlike usual magnetic systems, however, the T dependence is mostly due to the change of the volume fraction V_M .

The internal field at the muon site in HTSC systems is due to dipolar field from neighbouring static Cu spins. Depending on the range of this field, the volume fraction of muons V_M subject to static field is somewhat larger than the volume fraction V_{Cu} of frozen Cu spins. Figure 8(a) shows our simulation results for the relationship between V_{Cu} and V_M for cases with incommensurate static magnetism in island regions having a radius R [10]. Here we see that about 70-80% population of static Cu spins is enough to create observable static fields at the sites of all the muons. Thus, our previous result [33] on $\text{La}_{1.45}\text{Nd}_{0.4}\text{Sr}_{0.15}\text{CuO}_4$ (LNSCO:0.15), which is a superconductor with $T_c \sim 10\text{K}$ with $V_M > 95\%$ is still compatible with a picture that superconductivity and static magnetism occur in mutually exclusive regions of CuO_2 plane.

Although the relationship between V_M and V_{Cu} is nearly independent of the radius R of static SDW islands, the damping rate Λ of the Bessel oscillation depends on R , as shown in Fig. 8(b). By converting observed V_M into V_{Cu} using Fig. 8(a), and then plotting observed Λ in Fig. 8(b), we find that our ZF- μ SR results in LCO:4.11 are consistent with the island size $R \sim 15 - 30 \text{ \AA}$ [10]. Note that this length scale is comparable to ξ_{ab} . This model of “static SDW nano islands” can be reconciled with the long range spin correlations found by neutron Bragg peaks, if we consider percolation of these islands via a help of interplaner correlations, as proposed in [10].

To study the relationship between the magnetic volume fraction V_{Cu} and the superfluid density n_s/m^* , we performed μ SR measurements in $(\text{La}_{1.85-y}\text{Eu}_y\text{Sr}_{0.15})\text{CuO}_4$ (LESCO) [11,34] where the concentration of doped hole carriers is fixed to 0.15 per Cu, while the magnetic volume changes with increasing Eu concentration y . The volume fraction with static magnetism was determined

by the ZF- μ SR, while n_s/m^* was measured in TF- μ SR. The results shown in Fig. 9 clearly demonstrate a trade-off between V_{Cu} and the superfluid density n_s/m^* . This implies that superconductivity does not exist in the volume which has static magnetism.

In the plot of $\sigma(T \rightarrow 0)$ versus T_c in Fig. 1, the results of these systems with static stripe magnetism, shown by the striped square symbols, follow the trajectory of simple hole-doped and Zn-doped systems. This indicates that n_s/m^* is again a determining factor of T_c in HTSC systems where superconductivity and magnetism coexist. We also note that the results in overdoped Tl2201 can be viewed as following a monotonic relationship between T_c and the superfluid density, with the slope roughly comparable to cuprates with/without other types of perturbations.

V. ANALOGY WITH SUPERFLUID HE FILMS

Superfluid He films represent another set of systems where T_c is strongly correlated with the 2-dimensional superfluid density n_{s2d} at $T \rightarrow 0$. Using the published results, we made Fig. 10 [35] which shows correlations between T_c and n_{s2d}/m^* for ^4He films on Mylar substrate (open circle symbol) [36], on Vycor Glass which represents a porous media (star symbol) [37,38], as well as for $^4\text{He}/^3\text{He}$ mixtures adsorbed on fine alumina powders (closed diamond symbol) [39]. The results on Mylar films show linear relationship, consistent with the behavior expected for the KT transition [40] (see next section for details) as indicated by the solid line. With the lowest level of perturbation, this case corresponds to simple hole-doped HTSC systems in comparison between the cuprates and He films. The results on Vycor Glass is analogous to the Zn-doped cuprates: in both cases some normal regions are formed as a “healing region/layer”, while T_c is still strongly correlated with the superfluid density despite non-trivial geometry of the superfluid.

Mixture of bosonic ^4He and fermionic ^3He liquids exhibits a phase diagram shown in the inset of Fig. 10. With increasing ^3He fraction, T_c decreases, being roughly proportional to the volume fraction of ^4He . In bulk geometry, the mixture undergoes macroscopic phase separation into ^4He -rich superfluid and ^3He -rich normal fluid, the heavier superfluid existing underneath the lighter normal fluid in a container. This phase separation can be confined into a microscopic length scale by adsorbing the mixture onto porous media or fine powders [39,41], where superfluidity remains up to a large ^3He fraction. The results for the $^4\text{He}/^3\text{He}$ mixture in Fig. 10 exhibit a behavior very similar to that of overdoped Tl2201 in the cuprates in Fig. 1. In both the He mixture and the overdoped HTSC, inclusion of too many fermions (doped holes and ^3He) results in microscopic phase separation and reduction of both T_c and the superfluid density. Thus, we find a remarkable similarities [35] in the

plot of T_c versus superfluid density in cuprates (Fig. 1) and He films (Fig. 10) for the cases with/without perturbation.

Figure 1 shows correlations between T_c and 3-dimensional (3-d) superfluid density while Fig. 10 shows T_c versus 2-d superfluid density. By knowing the average interlayer distance c_{int} between the CuO_2 planes, we can generate a plot of T_c versus n_{s2d}/m^* for the cuprate systems. The resulting plot, Fig. 11, clearly indicates that in HTSC systems, T_c is higher for shorter c_{int} for a given 2-d superfluid density n_{s2d}/m^* [42]. This observation is consistent with the variation of T_c reported for multilayer films with alternating layers of superconducting $\text{YBa}_2\text{Cu}_3\text{O}_7$ (YBCO) and insulating $\text{PrBa}_2\text{Cu}_3\text{O}_7$ (PBCO) [43], as shown in the inset of Fig. 11. These results indicate that the interlayer coupling is essential for obtaining higher T_c in HTSC systems. The observed variation of T_c cannot be explained by the simplest version of KT transition where T_c should be determined solely by n_{s2d}/m^* .

VI. CONDENSATION MECHANISMS

A. BE and BCS condensation and KT transition

Correlations between T_c and the superfluid density shown in Fig. 1 and Fig. 11 help consideration of condensation mechanisms in HTSC systems. In BE condensation [44], the bosons are pre-formed at a very high “paring” temperature T_p . At a given temperature $T < T_p$ each boson has kinetic energy of $k_B T$, which defines the thermal wave length λ_{th} representing the spread of the wave function of this boson due to the uncertainty principle. With decreasing T , λ_{th} increases. When λ_{th} becomes comparable to the inter-particle distance $n_B^{-1/3}$, the wave functions of neighbouring bosons start to overlap, as illustrated in Fig. 12(a). Thanks to the tendency of bosons to fall into the same state by building up phase coherence of wave functions, Bose condensation occurs at T where $\lambda_{th} \sim n_B^{-1/3}$. From this, we have the BE condensation temperature $T_B \propto n_B^{2/3}/m_B$, where n_B and m_B denote the density and mass of the boson. In this way, the superfluid density and T_c is directly related in BE condensation.

In BCS condensation [45], the energy scale of attractive interaction determines the energy gap and T_c . The effective Fermi energy $\epsilon_F \propto n_n^{2/3}/m^*$ is much larger than kT_c in BCS condensation, i.e., there is a sufficient density of fermions above T_c . However, the system stays in the normal state until the temperature is reduced to the pairing energy scale T_p , where bosons are formed. Once pairs are formed, their boson density is high enough at T_c , and thus the condensation occurs immediately at $T_c \sim T_p$. In BCS condensation, T_c depends on carrier density through the density of states at the Fermi level which determines the strength of electron-phonon interaction. However, this

dependence is rather indirect. Suppose we have a BCS superconductor with the carrier density n_s . If the Debye frequency is doubled, T_c and the energy gap Δ would be doubled. However the carrier density stays unchanged, as can be found from the illustration of Fig. 12(b). This example shows that the superfluid density is not a direct determining factor for T_c in BCS condensation.

Kosterlitz-Thouless transition [40] is a phenomenon in 2-dimensional superfluids / superconductors. The elementary excitation of superfluid He film is the formation of vortex anti-vortex pairs. The energy required for this is governed by the phase stiffness, which is proportional to the superfluid density. At the transition temperature T_{KT} , the thermal energy becomes sufficient to form unbound vortices, which results in dissipation and destruction of superfluidity / phase coherence. Thermodynamic arguments lead to the universal relationship between the 2-d superfluid density at $T = T_{KT}$ and the value of T_c as $kT_{KT} \propto n_{s2d}/m^*(T = T_{KT})$, which should be independent of material. This relationship was confirmed as the jump of the superfluid density at the superfluid transition of He films [46].

B. Evolution from 3-d to 2-d

Figure 13(a) illustrates evolution of various energy scales in superfluid He film and a thin film of BCS superconductor. The BE condensation temperature of He in the 3-d limit corresponds to the lambda temperature $T_\lambda = 2.2$ K, which is close to $T_B \propto n_B^{2/3}/m^*$, except for some reduction due to departure of real system from an ideal non-interacting Bose-gas limit. With decreasing film thickness d , T_c starts to change when the thickness becomes comparable to a few times the coherence length $\xi \sim n_B^{-1/3}$. For $d \leq \xi$, $T_c \propto n_{s2d}/m^*$. In superfluid He film on Mylar, the superfluid density at $T \rightarrow 0$ is very close to that at just below T_c , as shown in Fig. 13(a). Thus the Kosterlitz-Thouless relation holds for n_{s2d} at $T \rightarrow 0$, as can be seen in Fig. 10. Between T_c and $T_\lambda = 2.2$ K, the order parameter exhibits phase fluctuations, i.e., superfluidity is dynamic. The pair formation energy scale is much higher than T_c in He for any thickness value d .

In a thin film of a BCS superconductor, T_c should show a similar reduction from the value T_{c3d} in the bulk 3-d system, when the film thickness becomes comparable to or smaller than a few times ξ in the clean limit (and l in the dirty limit), as shown in Fig. 13(b). The superfluid density n_s/m^* at $T \rightarrow 0$ would follow a thickness dependence similar to that of T_c . Note that n_s/m^* is very large, as it is related to $T_F \propto n_n^{2/3}/m^* \gg T_c$ in the 3-d limit. There should be difference between n_n/m^* and n_s/m^* in the region $d < \xi$ (or l), due to difficulty in forming pairs in a restricted geometry. On the other hand, the general argument of KT relationship should still hold. This is possible only if n_{s2d}/m^* at $T = T_c$ for $d < \xi$

is much smaller than n_{s2d}/m^* at $T \rightarrow 0$, as illustrated in Fig. 13(b). Therefore, the “jump” of the superfluid density at T_{KT} is practically invisible in a BCS thin film. For $d \leq \xi$, the region $T_c < T < T_{c3d}$ is characterized by phase fluctuations. However, the pair formation occurs at $T \sim T_{c3d}$ for any thickness. Consequently, bosons exist only below T_{c3d} , as illustrated in Fig. 13(b).

C. BE-BCS Crossover and Phase Fluctuation Models

In 1989 [6] and 1991 [7], we suggested the relevance of BE condensation to the universal relationship between T_c and n_s/m^* in HTSC systems shown in Fig. 1 [6]. By combining this phenomenon with the pseudogap behavior then observed by NMR and conductivity, we proposed a picture of BE to BCS crossover in 1993-94 [47,48], as illustrated in Fig. 14(a) [42,47,48]. General concept of the BE-BCS crossover has been considered earlier by several scientists [49], including Randeria and co-workers [50] who adopted this concept to the interpretation of the susceptibility/NMR results for the pseudo gap. Within our knowledge, however, our proposal was the first to combine the results of superfluid density with the pseudogap behavior in the underdoped cuprates. As shown in Fig. 14(a), we regarded the pseudogap temperature T^* as the pair formation temperature T_p . The reduction of the c-axis dc conductivity below T^* can be interpreted as resulting from reduced interplaner tunneling probability for paired bosonic carriers having 2e charges, while reduction of magnetic susceptibility can be attributed to the formation of a spin singlet bosonic (pairing) state in this picture.

In 1995, Emery and Kivelson (EK) [51] proposed a model based on phase fluctuations, as illustrated in Fig. 14(b). The BE-BCS model and the phase fluctuation model share many features in common. However, there are several important differences. Based on the linear relationship between T_c and the superfluid density at $T \rightarrow 0$, EK presented arguments basically parallel to that for the KT transition in 2-d systems. They pointed out that T_c of the underdoped cuprates is determined by the energy scale for the phase fluctuations. In their picture, the entire region of pseudogap below T^* is characterized by phase fluctuations. They argued that the 2-dimensional aspect is essential for obtaining high T_c .

In order to calculate T_θ^{max} which denotes the energy scale for phase fluctuations to destroy superconductivity, EK multiplied $\lambda^{-2} \propto n_s/m^*$ to the interplaner distance c_{int} for HTSC and some other 2-d systems. This is equivalent of obtaining $n_{s2d}/m^* \propto T_F$ in 2-d. For 3-d systems, EK multiplied n_s/m^* and the coherence length ξ , which leads to an energy scale much higher than T_F . This energy scale is unrealistically high, and irrelevant to condensation arguments. If one substitutes the interparticle distance $n_s^{-1/3}$ instead of ξ , we recover T_F for 3-d

systems. Then, Table 1 in ref [51] by EK becomes essentially equivalent to Fig. 3 of our 1991 paper [7], shown as a part of Fig. 3 of this article, where we plotted T_c versus T_F . We consider that the distinction between 2-d and 3-d systems by EK is an artefact resulting from the overestimate of T_θ^{max} in 3-d systems. In general, the 2-dimensional aspect does not help increasing T_c of any superconductor, as can be found in Fig. 13.

Figure 15 shows the current estimates of T^* from various methods as plotted versus hole concentration. If the entire region below T^* is supposed to have superconducting phase fluctuations, as conjectured by EK, the situation is rather similar to a thin-film BCS superconductor shown in Fig. 13(b). In contrast, if T^* is solely representing the pair formation, as proposed in our BE-BCS crossover picture, and if there is a 2-dimensional aspect remaining in HTSC systems, there should be two different energy scales above T_c , as we discussed in ref [35]. They are the temperature T_{dyn} at which the phase coherence of bosons completely disappear and dynamic superconductivity vanishes, in addition to the temperature T_p at which pairs are dissolved into fermions. This situation is similar to the case of He films shown in Fig. 13(a). One of important differences between BE-BCS and EK conjectures lies in this point.

D. Pair formation and dynamic superconductivity

Since high- T_c cuprates have a highly 2-dimensional electronic structure, several experiments have detected the “dynamic superconductivity” existing above T_c : (1) In YBCO-PBCO films with a thick PBCO layers separating a single layer YBCO, T_c is reduced to 15-20 K. Between this temperature and the $T_c \sim 90$ K of the bulk YBCO, one observes reduction of the normal state conductivity, which follows the predictions of the Kosterlitz-Thouless theory [52]. (2) Corson *et al.* [53] measured dynamic superfluid response in underdoped Bi2212, and found that the response depends on the measuring frequency ω above a certain “branch-off” temperature T_{off} , as shown in Fig. 16. Furthermore, the superfluid density n_s/m^* at $T = T_{off}$ agrees well with the universal value $n_s/m^*(T = T_{KT})$ expected for the KT transition. The critical temperature T_c , at which $n_s/m^* = 0$, increases with increasing ω , suggesting that this phenomenon corresponds to the “dynamic superfluidity” expected above $T_c(\omega = 0)$ and below T_{dyn} . It should be noted, however, that T_{dyn} for the measuring frequency of 600 GHz is limited to $T \leq 100$ K.

These results indicate that certain cuprate systems with high anisotropy, such as underdoped Bi2212 and single-layer YBCO film, exhibit dynamic superconductivity as expected from the KT theory. However, these results do not necessarily provide explanation to the origin of the pseudo gap at $T = T^*$, since T_{dyn} observed in Bi2212 is significantly lower than the pseudo-gap temper-

ature T^* . Namely, the phase fluctuations alone cannot explain the entire pseudo-gap phenomena.

Dependence to an external magnetic field should be quite different if these two distinct energy scales above T_c correspond respectively to pairing and dynamic superconductivity. The former would not depend much on external fields, while the latter should be very sensitive to the field. Indeed, the pseudo gap below T^* was found to be insensitive to the applied field in tunneling measurements [54]. Recently, Lavrov *et al.* [55] found that c-axis conductivity shows negative magneto-resistance upon cooling at a temperature well below T^* but above T_c . This negative magneto-resistance may be due to the onset of dynamic superconductivity below T_{dyn} .

The results of the Nernst effect [56], which appear in the underdoped region of La214 systems above T_c but well below T^* can also be interpreted as possible evidence for dynamic superconductivity below T_{dyn} . Other phenomena potentially related to this energy scale include: (a) superfluid response of the ARPES coherence peak [57]; and (b) 41 meV neutron resonance mode [58].

Based on these considerations, we propose a new phase diagram, with two distinct lines of T^* and T_{dyn} in the underdoped region as shown in Fig. 17. Note that the pair formation at T^* is necessary for superconductivity in cuprates, but is not enough to support any phase coherence. It is only when the thermal energy scale becomes less than the energy scale representing the number density of bosons that the phase coherence can set in. The onset temperature T_{dyn} of dynamic superfluidity represents this energy scale. In highly 2-dimensional cases, one should further cool down below T_{dyn} before achieving long-range phase coherence at T_c .

VII. EVOLUTION FROM SUPERCONDUCTOR TO NORMAL METAL

A. phase diagram for the overdoped cuprates

In BCS superconductors in the clean limit, all the carriers in the Fermi sphere contribute to superfluid. There should be no normal carriers remaining at $T \rightarrow 0$. Therefore, neither the BE-BCS nor the phase fluctuation pictures can explain the reduction of n_s with increasing hole doping observed in several overdoped cuprate systems [8,15,25] described in section III-B.

Tallon, Loram and co-workers [59] have noticed that the T^* line may be heading towards $T = 0$ at a “critical hole concentration” around $x_c \sim 0.19$. μ SR studies of Panagopoulos *et al.* [60] show that static magnetism, either spontaneously existing or induced by Zn doping, disappears at $x \geq x_c$. Generally, increasing hole doping would tend to destroy magnetic interactions in the cuprates.

Let us make the following three assumptions: (a) the pairing in HTSC systems is due to a magnetic interaction; (b) the T^* line represents the pair formation, and (c) the T^* line disappears at $x = x_c$. Then, no genuine superconducting pairing exists in the overdoped region at $x \geq x_c$. However, if the energy loss for charge disproportionation is overcome by the gain of pairing and condensation energies, the system can spontaneously phase separate into a “hole-poor” superfluid with the local hole concentration $x \leq x_c$ and a “hole-rich” normal fermion region with $x > x_c$. If this phase separation remains microscopic with the length scale comparable to ξ_{ab} , we can expect superconductivity in the overdoped region, similarly to the case of $^4\text{He}/^3\text{He}$ mixture.

The energy loss of charge disproportionation can be estimated following Coulomb blockade type calculation and/or formation of nano-islands serving as capacitor allays. Our crude estimate [23] shows that this energy becomes comparable to pairing/condensation energy gain in the cuprates. Based on these considerations, we proposed a phase diagram shown in Fig. 17, with phase separation in the overdoped region. As shown in Fig. 5(b), the doping evolution of the superfluid density n_s , calculated using this model [23], shows a good qualitative agreement with the observed results. We also note that this model can reproduce a very sharp temperature dependence of n_s/m^* and H_{c2} at $T \rightarrow 0$ found in the heavily overdoped region of Tl2201 [8,15,61].

Tallon and Loram [59] presented a view that the existence of superconductivity in the overdoped cuprates at $x \geq x_c$, where the T^* line does not exist, implies that the magnetic interaction below the T^* line is not required for superconductivity but rather is a competing factor which weakens superconductivity. The present model with phase separation provides an alternative view where the pseudogap phenomena, as a necessary factor (pair formation) for superconductivity, can be compatible with superconductivity in the overdoped cuprates.

B. analogous cases in other systems

In HTSC cuprates, as well as in 2-d organic (BEDT-TTF)₂-X and 3-d A₃C₆₀ superconductors, superconductivity appears in the vicinity of the insulator to metal transition. Superconductivity is taken over by a presumably Fermi-liquid metallic state by increasing carrier doping in cuprates, or by application of chemical and/or external pressure in BEDT and A₃C₆₀. In all these cases, we expect that the normal state spectral density (or Drude weight) n_n/m^* to increase in the process towards a simple Fermi liquid. We showed that the superconducting spectral weight *decreases* in this process for the case of cuprates.

We performed magnetization measurements of the in-plane penetration depth in (BEDT-TTF)₂Cu(NCS)₂ under applied pressure [62], and found that n_s/m^* decreases

with increasing pressure as shown in Fig. 18(a), contrary to the behavior of n_n/m^* found in quantum oscillation measurements [63]. This system is known to be well in the clean limit. These results indicate that not only in cuprates but also in BEDT, the crossover from superconducting to metallic ground state is associated with anomalous reduction of the superfluid spectral weight.

Similar behavior is also seen in A_3C_{60} systems. As shown in Fig. 1 and Fig. 18(b), the muon relaxation rate $\sigma(T \rightarrow 0)$ measured in A_3C_{60} decreases with decreasing lattice constant [17,18], in the approach towards a simple metallic state. In view of rather large residual resistivity in the normal state, the results for these fullerides might be subject to correction related to the mean free path. However, the un-corrected raw data indicate that $1/\lambda^2$ again shows anomalous reduction when the system approaches presumably a simple metallic ground state.

These three systems exhibit similar phase diagrams: superconductivity appears in the evolution from magnetic and insulating ground state to presumably simple Fermi liquid state; in BEDT systems, a pseudo-gap like behavior near the magnetic phase was found in susceptibility. These features suggest a possibility that the anomalous results in the overdoped cuprates may be a generic behavior shared by a wider range of superconductors based on correlated electron systems. We note that all these systems follow the universal linear relationship in the plot of T_c versus n_s/m^* , with approximately the same slope as shown in Fig. 1 and in ref. [62].

VIII. SUMMARY

In this paper, we showed that T_c in HTSC cuprate systems exhibits universal correlations with the superfluid spectral weight n_s/m^* , for the cases of simple hole doping, as well as for more complicated cases with Zn-doping, overdoping and static SDW nano island formation, where the system undergoes spontaneous phase separation between superconducting and normal regions with the length scale comparable to the in-plane coherence length. Robustness of this relation for the case with/without perturbation is analogous to the case of superfluid ^4He and $^4\text{He}/^3\text{He}$ mixture films in non-porous and porous media. In all these cases, the superfluid density is the determining factor for T_c . This is the basic feature of BE condensation.

By slightly revising the BE-BCS crossover picture, we have proposed a new phase diagram for the cuprates which has (a) two separate lines of T^* and T_{dyn} above T_c in the pseudogap state in the underdoped region, (b) disappearance of the T^* line at the critical hole concentration x_c , and (c) phase separation in the overdoped region. In this model, the T^* line represents pair formation, whereas the T_{dyn} line corresponds to the onset of dynamic superconductivity. Low dimensionality prevents formation of long-range phase coherence between T_{dyn}

and T_c . We also noted anomalous reduction of the superfluid spectral weight n_s/m^* in the overdoped cuprates as well as in the 2-d organic BEDT and 3-d fulleride superconductors, when the system approach simple metallic ground state.

IX. ACKNOWLEDGEMENT

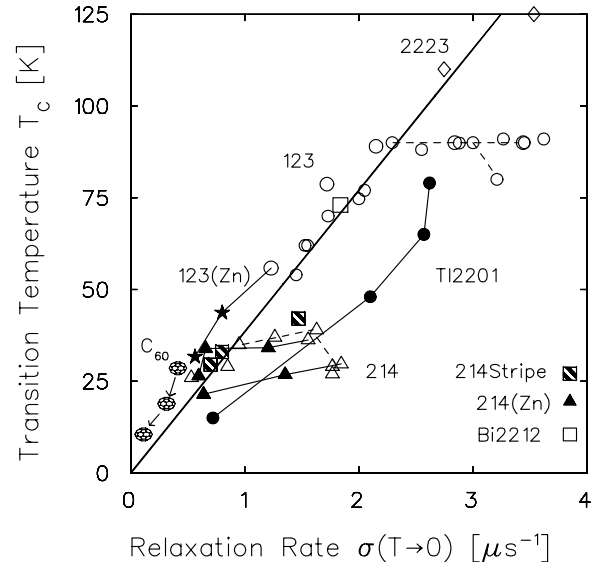
The author would like to acknowledge collaboration with G.M. Luke, K.M. Kojima, S. Uchida, R.J. Birge-neau, K. Yamada and discussions with O. Tchernyshyov and M. Randeria. This work is supported by a grant from US NSF DMR-01-02752 and CHE-01-17752.

-
- [1] For general aspects and historical development of μSR , see Proceedings of nine international conferences on muon spin rotation / relaxation/ resonance in *Hyperfine Interact.* **6** (1979); **8** (1981); **17-19** (1984); **31** (1986); **63-65** (1990); **85-87** (1994); **104-bf** 106 (1997); *Physica B* **289-290** (2000); and *Physica B* (Proceedings for μSR 2002, Williamsburg, Virginia, June, 2002), in press.
 - [2] For a general review of μSR , see, for example, A. Schenck, *Muon Spin Rotation Spectroscopy*, Adam Hilger, Bristol, 1985.
 - [3] For a recent reviews of μSR studies in topical subjects, see *Muon Science: Muons in Physics, Chemistry and Materials*, Proceedings of the Fifty First Scottish Universities Summer School in Physics, st. Andrews, August, 1988, ed. by S.L. Lee, S.H. Kilcoyne, and R. Cywinski, Inst. of Physics Publishing, Bristol, 1999.
 - [4] J.E. Sonier, J.H. Brewer, R.F. Kiefl, *μSR Studies of the Vortex State in Type-II Superconductors*, *Rev. Mod. Phys.* **72** (2002) 769.
 - [5] W. Barford and J.M.F. Gunn, *The theory of the measurements of the London penetration depth in uniaxial type-II superconductors by muon spin rotation*, *Physica C* **156** (1988) 515.
 - [6] Y.J. Uemura, G.M. Luke, B.J. Sternlieb, J.H. Brewer, J.F. Carolan, W.N. Hardy, R. Kadono, J.R. Kempton, R.F. Kiefl, S.R. Kreitzman, P. Mulhern, T.M. Riseman, D.Ll. Williams, B.X. Yang, S. Uchida, H. Takagi, J. Gopalakrishnan, A.W. Sleight, M.A. Subramanian, C.L. Chien, M.Z. Cieplak, Gang Xiao, V.Y. Lee, B.W. Statt, C.E. Stronach, W.J. Kossler, and X.H. Yu, *Universal Correlations between T_c and n_s/m^* (Carrier Density over Effective Mass) in High- T_c Cuprate Superconductors*, *Phys. Rev. Lett.* **62**, (1989) 2317.
 - [7] Y.J. Uemura, L.P. Le, G.M. Luke, B.J. Sternlieb, W.D. Wu, J.H. Brewer, T.M. Riseman, C.L. Seaman, M.B. Maple, M. Ishikawa, D.G. Hinks, J.D. Jorgensen, G. Saito, and H. Yamochi, *Basic Similarities among Cuprate, Bithmuthate, Organic, Chevrel-Phase and Heavy-Fermion Superconductors Shown by Penetration-Depth Measurements*, *Phys. Rev. Lett.* **66**, (1991) 2665.

- [8] Y.J. Uemura, A. Keren, L.P. Le, G.M. Luke, W.D. Wu, Y. Kubo, T. Manako, Y. Shimakawa, M. Subramanian, J.L. Cobb, and J.T. Markert, *Magnetic Field Penetration Depth in $Tl_2Ba_2CuO_{6+\delta}$ in the Overdoped Regime*, Nature (London) **364** (1993) 605.
- [9] B. Nachumi, A. Keren, K. Kojima, M. Larkin, G.M. Luke, J. Merrin, O. Tchernyshov, Y.J. Uemura, N. Ichikawa, M. Goto, and S. Uchida, *Muon Spin Relaxation Studies of Zn-Substitution Effects in High- T_c Cuprate Superconductors*, Phys. Rev. Lett. **77** (1996) 5421.
- [10] A.T. Savici, Y. Fudamoto, I.M. Gat, T. Ito, M.I. Larkin, Y.J. Uemura, G.M. Luke, K.M. Kojima, Y.S. Lee, M.A. Kastner, R.J. Birgeneau, K. Yamada, *Muon spin relaxation studies of incommensurate magnetism and superconductivity in stage-4 $La_2CuO_{4.11}$ and $La_{1.88}Sr_{0.12}CuO_4$* , Phys. Rev. **B66** (2002) 014524.
- [11] K.M. Kojima, S. Uchida, Y. Fudamoto, I.M. Gat, M.I. Larkin, Y.J. Uemura, G.M. Luke, *Superfluid density and volume fraction of static magnetism in stripe-stabilized $La_{1.85-y}Cu_ySr_{0.15}CuO_4$* , Proceedings of μ SR2002, Physica **B**, in press.
- [12] B. Pümpin, H. Keller, W. Kündig, I.M. Savić, J.W. Schneider, H. Simmer, P. Zimmermann, E. Kaldis, S. Rusiecki, C. Rossel, *μ SR in oxygen deficient $YBa_2Cu_3O_x$ ($6.5 \leq x \leq 7.0$)*, Hyperfine Interact. **63** (1990) 25.
- [13] C.L. Seaman, J.J. Neumeier, M.B. Maple, L.P. Le, G.M. Luke, B.J. Sternlieb, Y.J. Uemura, J.H. Brewer, R. Kadono, R.F. Kiefl, S.R. Kreitzman, T.M. Riseman, *Magnetic penetration depth of $Y_{1-x}Pr_xBa_2Cu_3O_{6.97}$ measured by muon-spin relaxation*, Phys. Rev. **B42** (1990) 6801.
- [14] J.L. Tallon, C. Bernhard, U. Binniger, A. Hofer, G.V.M. Williams, E.J. Ansaldo, J.I. Budnick, Ch. Niedermayer, *In-Plane Anisotropy of the Penetration Depth Due to Superconductivity on the Cu-O Chains in $YBa_2Cu_3O_{7-\delta}$, $Y_2Ba_4Cu_7O_{15-\delta}$, and $YBa_2Cu_4O_8$* Phys. Rev. Lett. **74** (1995) 1008.
- [15] Ch. Niedermayer, C. Bernhard, U. Binniger, H. Glücker, J.L. Tallon, E.J. Ansaldo, and J.I. Budnick, *Muon Spin Rotation Study of the Correlation Between T_c and n_s/m^* in Overdoped $Tl_2Ba_2CuO_{6+\delta}$* , Phys. Rev. Lett. **71** (1993) 1764.
- [16] A. Keren, A. Kanigel, J.S. Lord, A. Amato, *Superconductivity and magnetism in $(Ca_xLa_{1-x})(Ba_{1.75-x}La_{0.25+x})Cu_3O_y$: a μ SR investigation*, in this Proceedings, Solid State Comm.
- [17] Y.J. Uemura, A. Keren, G.M. Luke, L.P. Le, B.J. Sternlieb, W.D. Wu, J.H. Brewer, R.L. Whetten, S.M. Huang, Sophia Lin, R.B. Kaner, F. Diederich, S. Donovan, G. Grüner, K. Holczer, *Magnetic Field Penetration Depth in K_3C_{60} Measured by Muon Spin Relaxation*, Nature **352** (1991) 605.
- [18] Y.J. Uemura, A. Keren, L.P. Le, G.M. Luke, W.D. Wu, J.S. Tsai, K. Tanigaki, K. Holczer, S. Donovan, R.L. Whetten, *System Dependence of the Magnetic-field Penetration Depth in C_{60} Superconductors*, Physica **C235-240** (1994) 2501.
- [19] L.P. Le, G.M. Luke, B.J. Sternlieb, W.D. Wu, Y. J. Uemura, J.H. Brewer, T.M. Riseman, C. E. Stronach, G. Saito, H. Yamochi, H.H. Wang, A.M. Kimi, K.D. Carlson, J.M. Williams *Muon-spin-relaxation measurements of magnetic penetration depth in organic superconductors $(BEDT-TTF)_2-X$: $X=Cu(NCS)_2$ and $Cu[N(CN)_2]Br$* Phys. Rev. Lett. **68**, (1992) 1923.
- [20] Y.J. Uemura, Y. Fudamoto, I.M. Gat, M.I. Larkin, G.M. Luke, J. Merrin, K.M. Kojima, K. Itoh, S. Yamanaka, R.H. Heffner, D.E. MacLaughlin, *μ SR Studies of Intercalated $HfNCl$ Superconductors*, Physica **B289** (2000) 389.
- [21] S.H. Pan, E.W. Hudson, K.M. Lang, H. Eisaki, S. Uchida, J.C. Davis, *Imaging the Effects of Individual Zinc Impurity Atoms on Superconductivity in $Bi_2Sr_2CaCu_2O_{8+\delta}$* , Nature (London) **403** (2000) 746.
- [22] J.W. Loram, K.A. Mirza, J.M. Wada, J.R. Cooper, W.Y. Liang, *The electronic specific heat of cuprate superconductors*, Physica **C235-240** (1994) 134.
- [23] Y.J. Uemura, *Microscopic phase separation in the overdoped region of high- T_c cuprate superconductors*, Solid State Commun. **120** (2001) 347.
- [24] J. Schützmann, S. Tajima, S. Miyamoto, S. Tanaka, *c-Axis Optical Response of Fully Oxygenated $YBa_2Cu_3O_{7-\delta}$: Observation of Dirty-Limit-Like Superconductivity and Residual Unpaired Carriers*, Phys. Rev. Lett. **73** (1994) 174.
- [25] C. Bernhard, J.L. Tallon, Th. Blasius, A. Golnik, Ch. Niedermayer, *Anomalous Peak in the Superconducting Condensate Density of Cuprate High- T_c Superconductors at a Unique Doping State*, Phys. Rev. Lett. **86** (2001) 1614.
- [26] Y.J. Uemura, W.J. Kossler, X.H. Yu, J.R. Kempton, H.E. Schone, D. Opie, C.E. Stronach, D.C. Johnston, M.S. Alvarez, D.P. Goshorn, *Antiferromagnetism of La_2CuO_{4-y} Studied by Muon Spin Rotation*, Phys. Rev. Lett. **59** (1987) 1045.
- [27] J.M. Tranquada, B.J. Sternlieb, J.D. Axe, Y. Nakamura, S. Uchida, *Evidence for Stripe Correlations of Spins and Holes in Copper Oxide Superconductors*, Nature **375** (1995) 561.
- [28] G.M. Luke, L.P. Le, B.J. Sternlieb, W.D. Wu, Y.J. Uemura, J.H. Brewer, T.M. Riseman, S. Ishibashi, S. Uchida, *Static Magnetic Order in $La_{1.875}Ba_{0.125}CuO_4$* , Physica **C185-189** (1991) 1175.
- [29] L.P. Le, A. Keren, G.M. Luke, B.J. Sternlieb, W.D. Wu, Y.J. Uemura, J.H. Brewer, T.M. Riseman, R.V. Upasani, L.Y. Chiang, W. Kang, P.M. Chaikin, T. Csiba, G. Grüner, *Muon Spin Rotation/Relaxation Studies in $(TMTSF)_2-X$ Compounds*, Phys. Rev. **B48** (1993) 7284.
- [30] L.P. Le, R.H. Heffner, J.D. Thompson, G.J. Nieuwenhuys, D.E. Maclaughlin, P.C. Canfield, B.K. Chyo, A. Amato, R. Feyerherm, F.N. Gyax, A. Schenck, *μ SR studies of borocarbides*, Hyperfine Interact. **104** (1997) 49.
- [31] Y.S. Lee, R.J. Birgeneau, M.A. Kastner, Y. Endoh, S. Wakimoto, K. Yamada, R.W. Erwin, S.H. Lee, G. Shirane, *Neutron-scattering Study of Spin-density Wave Order in the Superconducting State of Excess Oxygen-doped La_2CuO_{4+y}* , Phys. Rev. **B60** (1999) 3643.
- [32] A.T. Savici, Y. Fudamoto, I.M. Gat, M.I. Larkin, Y.J. Uemura, K.M. Kojima, Y.S. Lee, M.A. Kastner, R.J. Birgeneau, *Static Magnetism in Superconducting Stage-4 La_2CuO_{4+y}* Physica **B289-290** (2000) 338.
- [33] B. Nachumi, Y. Fudamoto, A. Keren, K.M. Kojima,

- M. Larkin, G.M. Luke, J. Merrin, O. Tchernyshyov, Y.J. Uemura, N. Ichikawa, M. Goto, H. Takagi, S. Uchida, M.K. Crawford, E.M. McCarron, D.E. MacLaughlin, R.H. Heffner, *Muon Spin Relaxation Study of the Stripe Phase Order in $La_{1.6-x}Nd_{0.4}Sr_xCu_2O_4$ and Related 214 Cuprates* Phys. Rev. **B58** (1998) 8760.
- [34] K.M. Kojima, H. Eisaki, S. Uchida, Y. Fudamoto, I.M. Gat, A. Kinkhabwara, M.I. Larkin, G.M. Luke, Y.J. Uemura, *Magnetism and Superconductivity of High- T_c Cuprates (La, Eu, Sr) $_2CuO_4$* , Physica **B289** (2000) 373.
- [35] Y.J. Uemura, *What can we learn from comparison between cuprates and He Films?: Phase separation and fluctuating superconductivity*, Int. J. Mod. Phys. **B14** (2000) 3003.
- [36] G. Agnolet, D.F. McQueeney, J.D. Reppy, *Kosterlitz-Thouless Transition in Helium Films*, Phys. Rev. **B39** (1989) 8934.
- [37] D.J. Bishop, J.E. Berthold, J.M. Parpia, J.D. Reppy, *Superfluid Density of Thin 4He Films Adsorbed in Porous Vicor Glass*, Phys. Rev. **B24** (1981) 5047.
- [38] P.A. Crowell, F.W. Van Keuls, J.D. Reppy, *Onset of Superfluidity in 4He Films Adsorbed on Disordered Substrates*, Phys. Rev. **B55** (1997) 12620.
- [39] H. Chyo and G.A. Williams, *Superfluid Phase Transition of 3He - 4He Mixture Films Adsorbed on Alumina Powder*, J. Low Temp. Phys. **110** (1998) 533.
- [40] J.M. Kosterlitz and D.J. Thouless, *Ordering, Metastability and Phase-Transitions in 2-Dimensional Systems*, J. Phys. **C: Solid State Phys.** **6**, (1973) 1181
- [41] M. Chan, N. Mulders, J. Reppy, *Helium in Aerogel*, Physics Today (August, 1996) 30.
- [42] Y.J. Uemura, *Bose-Einstein to BCS crossover picture for high- T_c cuprates*, Physica **C282-287** (1997) 194.
- [43] Ø. Fisher, J.M. Triscone, O. Brunner, L. Antognazza, M. Affronte, O. Eibit, L. Mi'eville, T. Boichat, M.G. Karkut, *Superconductivity in artificially grown copper-oxide superlattices*, Physics **B169** (1991) 116.
- [44] For recent progress in research of Bose Einstein condensation, see *Bose-Einstein Condensation*, ed. by A. Griffin, D.W. Snoke, S. Stringari, Cambridge University Press, Cambridge, 1995.
- [45] J. Bardeen, L.N. Cooper and J.R. Schrieffer, *Theory of Superconductivity*, Phys. Rev. **108** (1957) 1175.
- [46] D.J. Bishop and J.D. Reppy, *Study of superfluid transition in 2-dimensional He-4 films*, Phys. Rev. Lett. **40** (1978) 1727.
- [47] Y.J. Uemura, *Energy Scales of Exotic Superconductors, in Polarons and Bipolarons in High- T_c Superconductors and Related Materials*, Proceedings of the International Workshop on Polarons and Bipolarons in High- T_c Superconductors and Related Materials, Cambridge, UK, April, 1994, ed. by E. Salje, A.S. Alexandrov and Y. Liang, Cambridge University Press (1995), p.p. 453-460.
- [48] Y.J. Uemura, *Energy Scales of High- T_c Cuprates, Doped Fullerenes, and Other Exotic Superconductors*, Proceedings of International Symposium/Workshop on High- T_c Superconductivity and the C₆₀ Family, May 1994, Beijing, ed., by H.C. Ren, Gordon and Breach (New York), (1995), p.p. 113-142.
- [49] P. Nozières and S. Schmitt-Rink, *Bose condensation in an attractive Fermion Gas - From weak to strong coupling superconductivity* J. Low Temp. Phys. **59** (1985) 195.
- [50] M. Randeria, *Crossover from BCS theory to Bose-Einstein Condensation*, in *Bose-Einstein Condensation*, ed. by A. Griffin, D.W. Snoke, S. Stringari, Cambridge University Press, Cambridge, 1995, p.p. 355-391, and references therein.
- [51] V. Emery and S. Kivelson, *Importance of phase fluctuations in superconductors with small superfluid density*, Nature **374** (1995) 434.
- [52] M. Rasolt, T. Edis, Z. Tesanović, *Kosterlitz-Thouless Transition and Charge Redistribution in the Superconductivity of YBCO/PBCO Superlattices*, Phys. Rev. Lett. **66** (1991) 2927.
- [53] J. Corson, R. Mallozzi, J. Orenstein, J.N. Eckstein, I. Bozovic, *Vanishing of phase coherence in underdoped $Bi_2Sr_2CaCu_2O_{8+\delta}$* , Nature (London) **398** (1999) 221.
- [54] V.M. Kransov, A.E. Kovalev, A. Yurgens, D. Winkler, *Magnetic field dependence of superconducting gap and the Pseudogap in Bi2212 and HgBr₂-Bi2212 studied by intrinsic tunneling spectroscopy*, Phys. Rev. Lett. **86** (2001) 2657.
- [55] A.N. Lavrov, Y. Ando, S. Ono, *Two mechanisms of pseudogap formation in Bi2201: Evidence from the c-axis magnetoresistance*, Eyrrophys. Lett. **57** (2002) 267.
- [56] Z.A. Xu, N.P. Ong, Y. Wang, T. Kakeshita, S. Uchida, *Vortex-like excitations and the onset of superconducting phase fluctuation in underdoped $La_{2-x}Sr_xCuO_4$* , Nature **406** (2000) 486.
- [57] D.L. Feng, D.H. Lu, K.M. Shen, C. Kim, H. Eisaki, A. Damascelli, R. Yoshizaki, J. Shimoyama, K. Kishio, G.D. Gu, S. Oh, A. Andrus, J. O'Donnell, J.N. Eckstein, Z.X. Shen, *Signature of superfluid density in the single-particle excitation spectrum of $Bi_2Sr_2CaCu_2O_{8+\delta}$* , Science **289** (2000) 277.
- [58] P.C. Dai, H.A. Mook, G. Aeppli, S.M. Hayden, F. Dogan, *Resonance as a measure of pairing correlations in the high- T_c superconductor $YBa_2Cu_3O_{6.6}$* , Nature **406** (2000) 965.
- [59] J.L. Tallon and J.W. Loram, *The doping dependence of T^* - what is the real high- T_c phase diagram?* Physica **C349** (2001) 53.
- [60] C. Panagopoulos, J.L. Tallon, B.D. Rainford, J.R. Cooper, C.A. Scott, T. Xiang *Low frequency spins and the ground state in high- T_c cuprates*, contribution to this Proceedings, Solid State Commun.
- [61] A.P. MacKenzie, S.R. Julian, G.G. Lonzarich, A. Carrington, S.D. Hughes, R.S. Liu, D.C. Sinclair, *Resistive upper critical-field of $Tl_2Ba_2CuO_6$ at low temperature and high magnetic-fields* Phys. Rev. Lett. **71** (1993) 1238.
- [62] M.I. Larkin, A. Kinkhabwala, Y.J. Uemura, Y. Sushko, G. Saito, *Pressure dependence of the magnetic penetration depth in κ -(BEDT-TTF) $_2Cu(NCS)_2$* , Phys. Rev. **B64** (2001) 144514.
- [63] J. Caulfield, W. Lubczynski, F.L. Pratt, J. Singleton, D.Y.K. Ko, W. Hayes, M. Kurmoo, P. Day, *Magneto-transport studies of the organic superconductor κ -(BEDT-TTF) $_2Cu(NCS)_2$ under pressure - the relationship between carrier effective-mass and critical temperature* J. Phys. Condens.-Matter **6** (1994) 2911.
- [64] A. Oshiyama and S. Saito, *Linear Dependence of Supercon-*

ducting Transition Temperature on Fermi-Level Density-of-States in Alkali-Doped C_{60} , Solid State Commun. **82** (1992) 41.



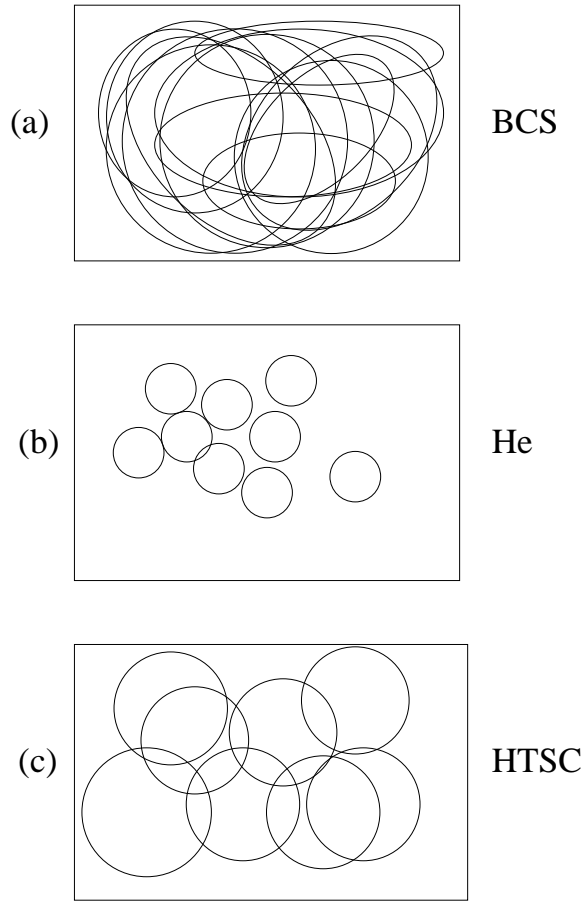


FIG. 2. Schematic view of overlap of pairs / bosons in (a) BCS superconductors, (b) superfluid ^4He , and (c) HTSC cuprate systems. The circles represent the size of the pair, whose length scale is given by the coherence length. We estimate that about 3 to 5 pairs are overlapping with one another in the HTSC systems. These results suggest that HTSC systems lie in crossover from BE to BCS condensation.

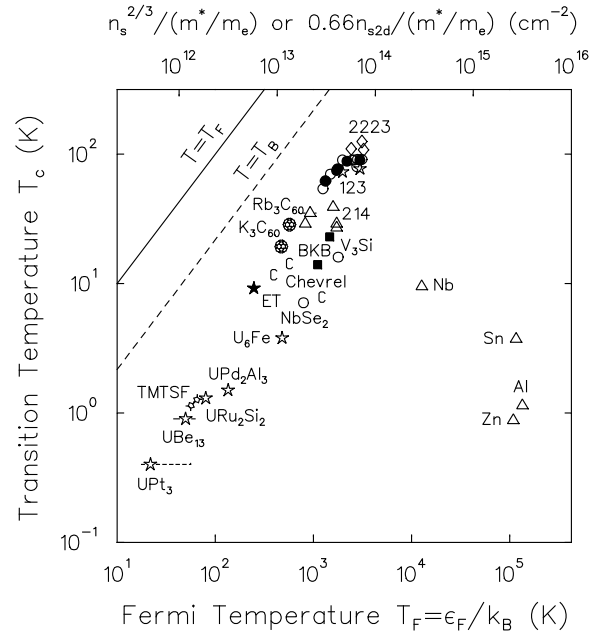


FIG. 3. A plot of T_c versus the effective Fermi temperature T_F obtained from the muon spin relaxation rate $\sigma(T \rightarrow 0)$ (in combination with the average interlayer distance c_{int} for 2-d systems, and with the Sommerfeld constant γ for 3-d systems) in various superconductors [7]. The broken line denotes Bose-Einstein condensation temperature T_B for a given boson density $n_s/2$ and mass $2m^*$.

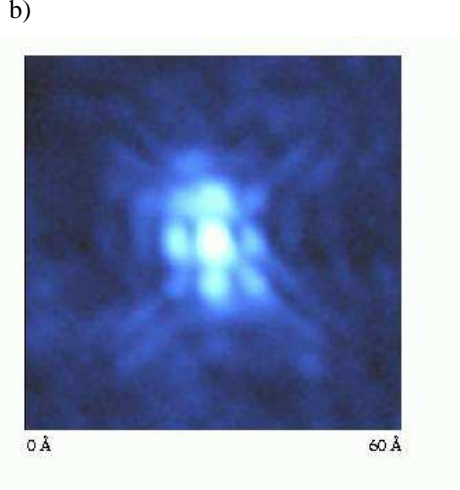
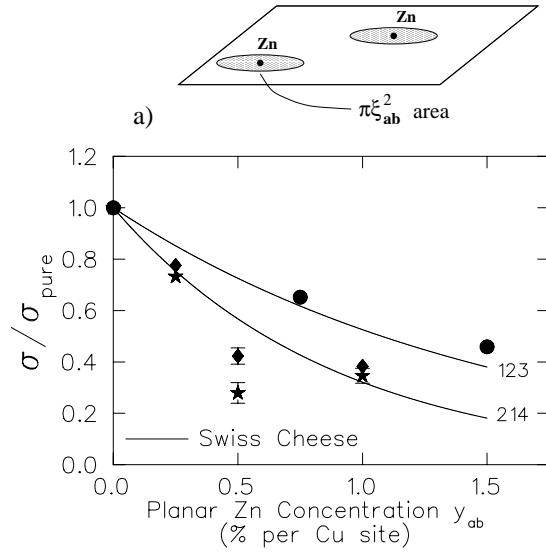


FIG. 4. (a) Muon spin relaxation rate $\sigma \propto n_s/m^*$ at $T \rightarrow 0$ plotted as a function of Zn concentration on the CuO₂ plane in YBa₂(Cu,Zn)₃O_{6.63} (123) (closed circle), La_{1.85}Sr_{0.15}(Cu,Zn)O₄ (closed diamond), and La_{1.8}Sr_{0.2}(Cu,Zn)O₄ (star symbol), together with the estimate of “Swiss Cheese model” illustrated in the top figure [9]. In this model, carriers in the shaded region around each Zn impurity do not contribute to the superfluid. (b) The local density of states (LDOS) profile obtained by Scanning Tunneling Microscope by Pan *et al.* in Bi₂212 around a Zn impurity [21]. The bright spot in the center corresponds to high density of states in the normal region, while the dark profile are from superconducting region with a gap in LDOS.

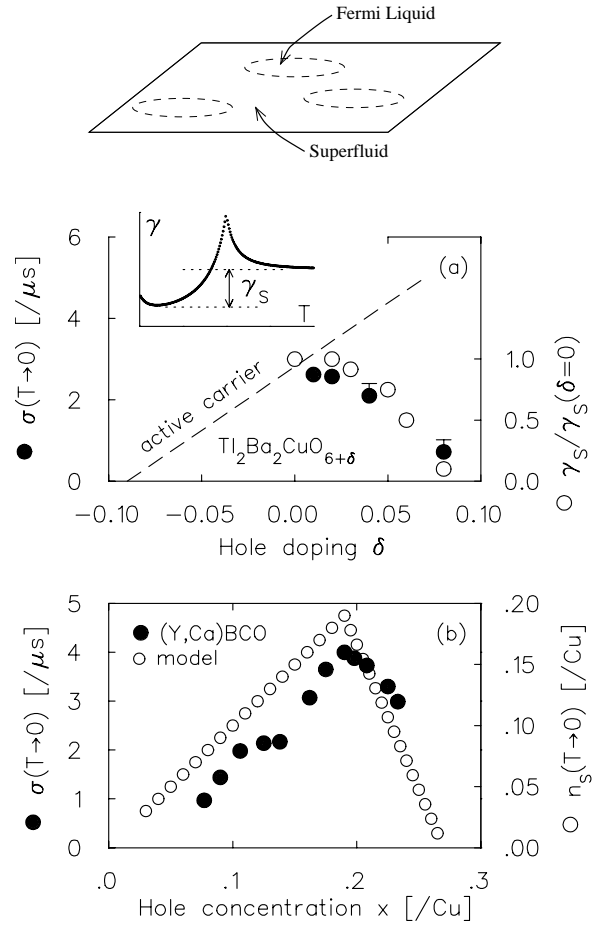


FIG. 5. (a) Muon spin relaxation rate $\sigma(T \rightarrow 0) \propto n_s/m^*$ (closed circles) [8] and the “gapped” response γ_s in the linear-term of the specific heat (open circles) [22] as a function of oxygen concentration in Tl₂Ba₂CuO_{6+ δ} (Tl2201). The broken line illustrates a projected variation of n_n/m^* . (b) Doping dependence of $\sigma(T \rightarrow 0) \propto n_s/m^*$ observed in (Y,Ca)Ba₂Cu₃O_y by Bernhard *et al.* [25] (closed circles) and the superfluid density $n_s(T \rightarrow 0)$ calculated for a simple model with microscopic phase separation in overdoped cuprates [23], as illustrated in the top figure.

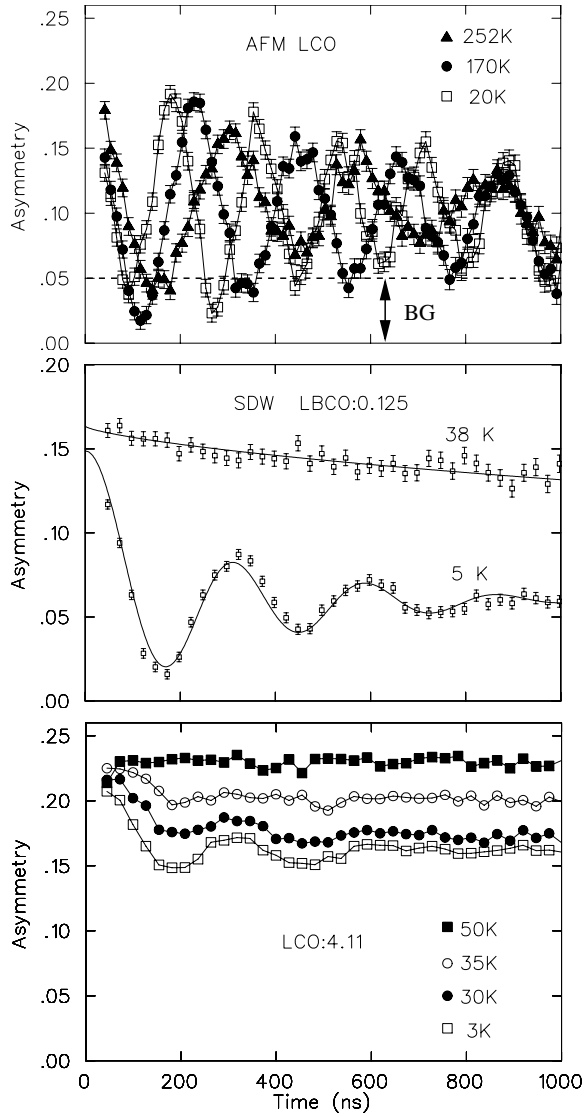


FIG. 6. Time spectra of ZF- μ SR measurements in (a) antiferromagnetic La_2CuO_4 (AF-LCO), (b) $\text{La}_{1.875}\text{Ba}_{0.125}\text{CuO}_4$ (LBCO:0.125) and (c) stage-4 $\text{La}_2\text{CuO}_{4.11}$ [10]. In AF-LCO, the oscillation amplitude below $T_N > 250$ K does not depend on T , while the frequency increases with decreasing T , reflecting build-up of sub-lattice magnetization. This is the behavior observed by μ SR in most of uniform ferro or antiferromagnetic systems. In LBCO:0.125 [28], we see a Bessel function form at $T = 5$ K, which is expected for the system with incommensurate static magnetism developed in the full volume fraction. In LCO:4.11, the amplitude of the oscillating and relaxing signal varies with T without much change in the frequency. The volume fraction of regions with static magnetism is less than a half even at $T \rightarrow 0$ [10].

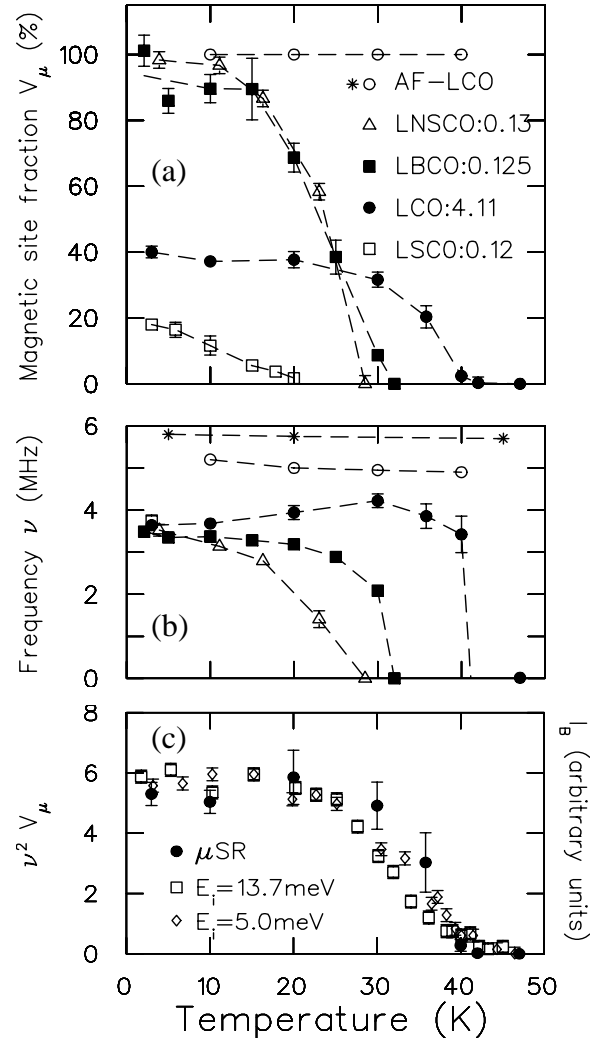


FIG. 7. (a) Volume fraction V_μ of muon sites with a static magnetic field larger than ~ 30 G and (b) frequency of the precessing signal in $\text{La}_2\text{CuO}_{4.11}$ (LCO:4.11) and $\text{La}_{1.88}\text{Sr}_{0.12}\text{CuO}_4$ (LSCO:0.12) ([10]), compared with the results in $\text{La}_{1.875}\text{Ba}_{0.125}\text{CuO}_4$ (LBCO:0.125) [28], $\text{La}_{1.47}\text{Nd}_{0.4}\text{Sr}_{0.13}\text{CuO}_4$ (LNSCO:0.13) [33], and antiferromagnetic $\text{La}_2\text{CuO}_{4+\delta}$ (AF-LCO) [26]. The broken lines are guides to the eye. (c) Comparison of the neutron Bragg peak intensity I_B in $\text{La}_2\text{CuO}_{4.11}$ (LCO:4.11) [31] with those expected from the μ SR results (present study) as $I_B \propto V_\mu \times \nu^2$. μ SR and neutron results are scaled using the values near $T \rightarrow 0$.

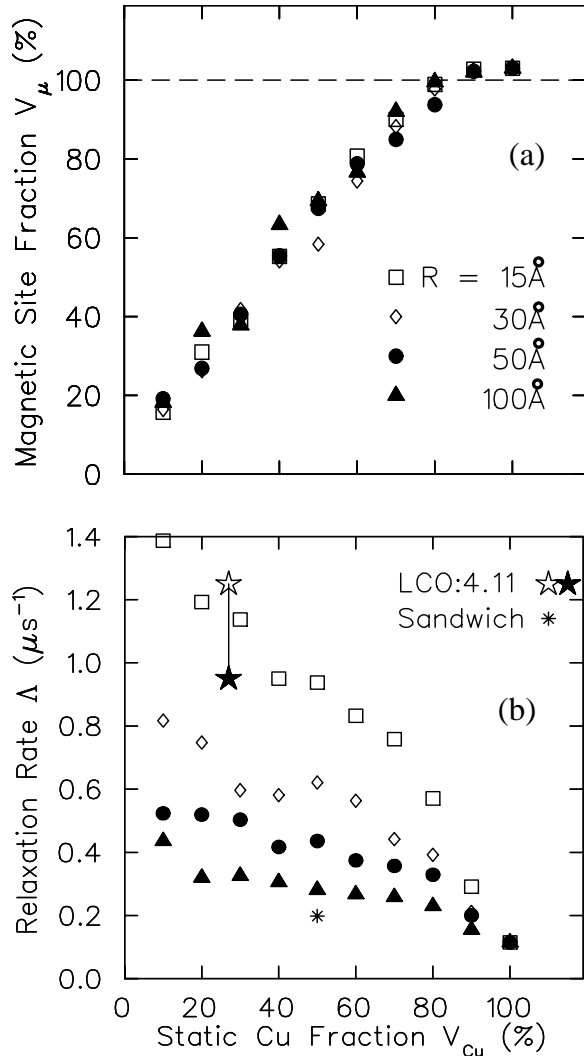


FIG. 8. (a) Computer simulation results for the volume fraction V_μ of muon sites with a static magnetic field larger than ~ 30 G as a function of the volume fraction of the sample containing static Cu moments, V_{Cu} . (b) The relaxation rate Λ of the Bessel function oscillation, obtained by fitting the simulation results with Eq. 3, plotted as a function of V_{Cu} . Comparison with the experimental results for LCO:4.11 (Raw data $\Lambda_{4.11}$ shown by an open star symbol and corrected data $\hat{\Lambda}_{4.11}$ by a closed star symbol) allows estimation of the size of magnetic islands to be about $R \sim 15 - 30$ Å. The asterisk symbol * shows the relaxation rate Λ expected for the sandwich model. See ref. [10] for details.

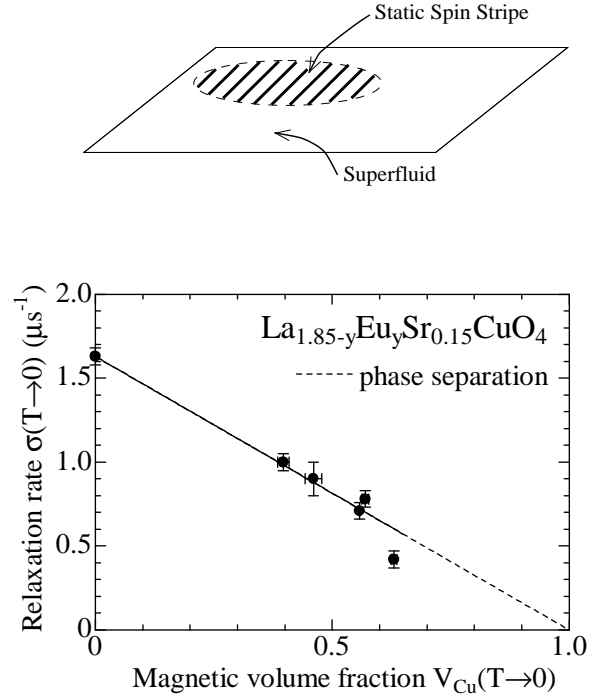


FIG. 9. Muon spin relaxation rate $\sigma(T \rightarrow 0)$ due to superconductivity observed in transverse-field μ SR measurements using ceramic specimens of $La_{1.85-y}Eu_ySr_{0.15}CuO_4$ (LESCO) by Kojima *et al.* [11], plotted against the volume fraction of static Cu moment V_{Cu} at $T \rightarrow 0$ determined by zero-field μ SR. The trade-off of these two parameters clearly demonstrates that superconductivity and static magnetism occur in mutually exclusive volume, as illustrated in the top figure.

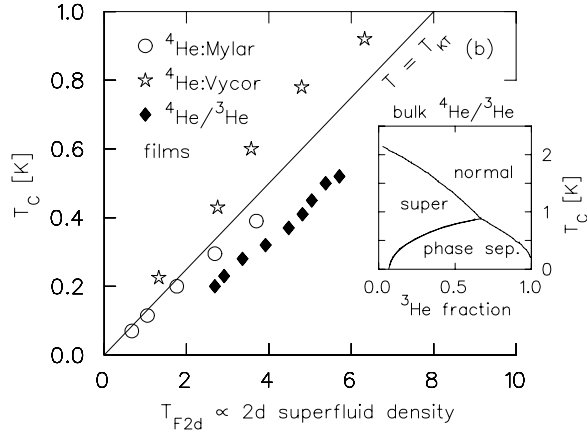


FIG. 10. Superfluid transition temperature T_c of ${}^4\text{He}$ films adsorbed on regular (Mylar) [36,37] and porous (Vycor glass) [38] media and ${}^4\text{He}/{}^3\text{He}$ films on fine Alumina powders [39], plotted against 2-dimensional superfluid density at $T \rightarrow 0$, after converted to the corresponding 2-dimensional Fermi temperature [23,35]. Inset figure shows the phase diagram of bulk ${}^4\text{He}/{}^3\text{He}$ mixture.

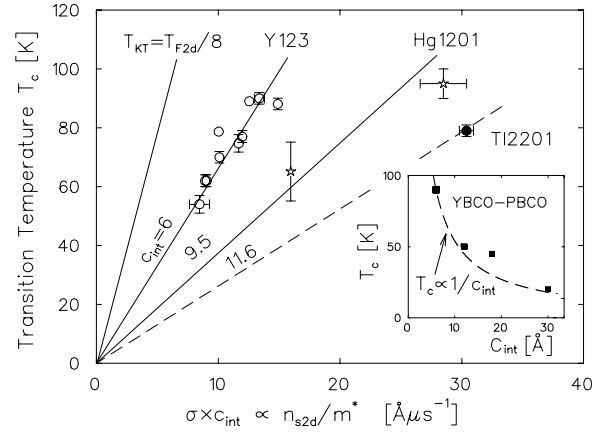


FIG. 11. Transition temperature T_c of HTSC cuprate superconductors plotted against the 2-dimensional superfluid density n_{s2d}/m^* obtained by multiplying the μSR relaxation rate σ with the average interplaner distance c_{int} between adjacent CuO_2 planes [41]. The inset figure shows variation of T_c with c_{int} in multi-layer films of YBCO/PBCO stacked along the c -axis direction [43]

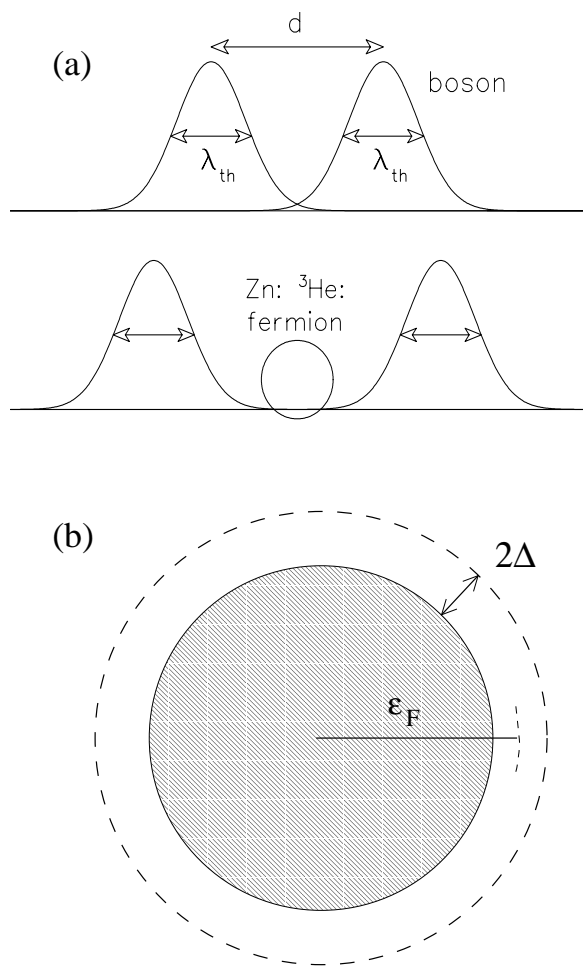
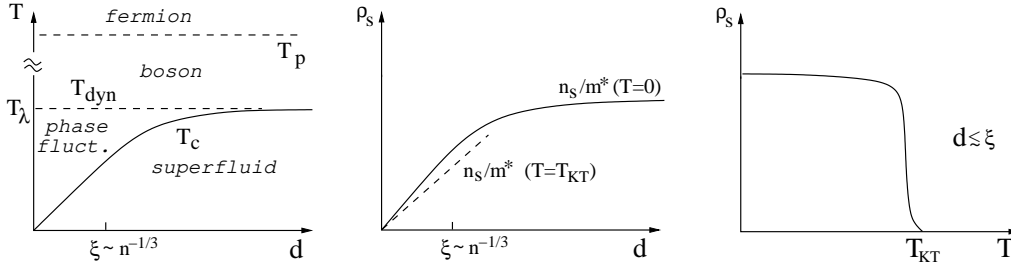


FIG. 12. (a) A schematic illustration of Bose-Einstein condensation, which occurs when the wave functions of neighbouring bosons, with the spread given by the thermal de-Broglie wave length λ_{th} , start to overlap. In this case T_c is directly related to the number density of bosons. (b) Fermi sphere and the energy gap in BCS superconductors. If one doubles the Debye frequency, the energy gap Δ and T_c would be doubled, while the superfluid density (all the carriers in the Fermi sphere) would be unchanged.

Superfluid He film



BCS thin film

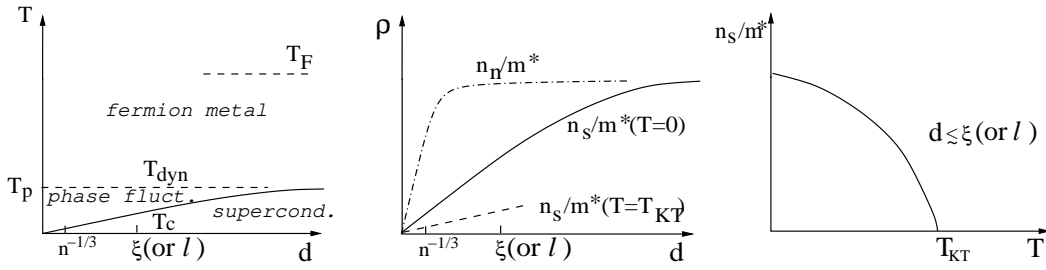


FIG. 13. Variation of pair-formation temperature scale T_p , the onset temperature T_{dyn} of superfluidity / superconductivity, the transition temperature T_c , and the superfluid density, as a function of film thickness d expected in (a) superfluid He film and (b) a thin film BCS superconductor. Also shown are temperature dependences of the superfluid density in the 2-d limit where the film thickness is comparable to or less than the coherence length

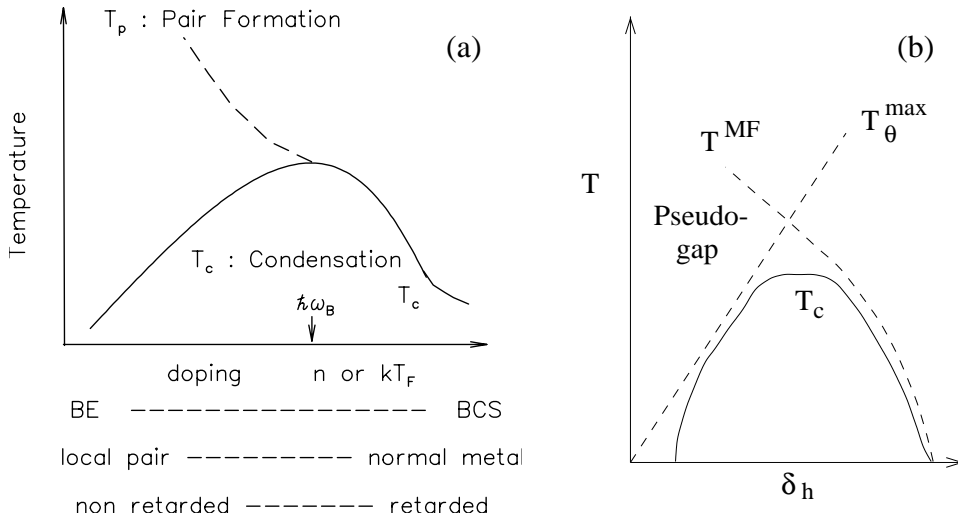


FIG. 14. Phase diagrams describing (a) the Bose-Einstein to BCS crossover picture proposed for HTSC systems by Uemura [47,48,42] and (b) the phase fluctuation picture proposed by Emery and Kivelson [51]

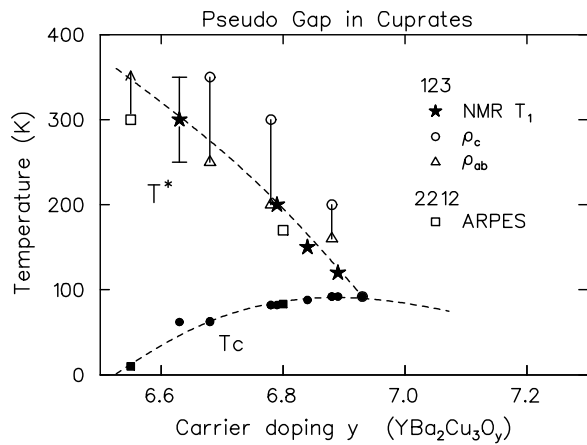


FIG. 15. Variation of the pseudogap temperature T^* and the superconducting transition temperature T_c , as a function of carrier doping, observed by several different experimental methods in the Y123 and Bi2212 systems.

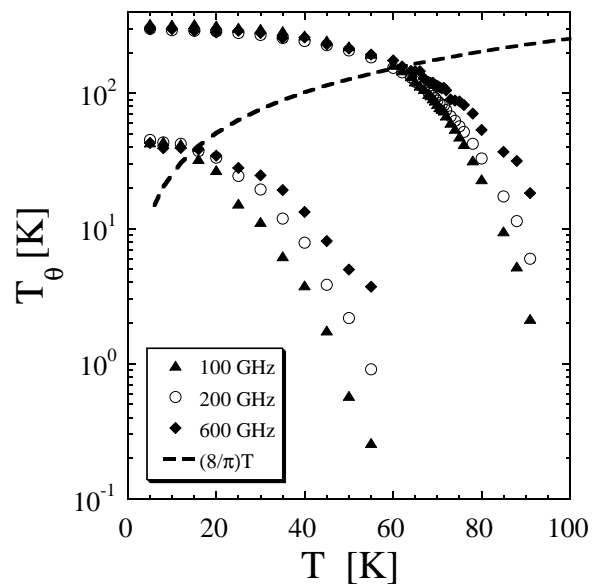


FIG. 16. Temperature dependence of the superfluid density observed in underdoped Bi2212 systems by high-frequency ac conductivity measurements of Corson *et al.* [53] with several different measuring frequencies. The broken line shows the universal relationship between the superfluid density at T_{KT} and the Kosterlitz-Thouless transition temperature T_{KT} .

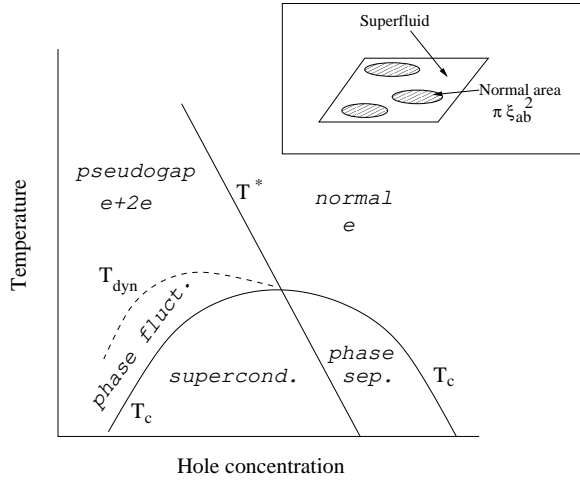


FIG. 17. A phase diagram for HTSC cuprates which involves (1) vanishing of the T^* line at a critical hole concentration; (2) T^* representing energy scale for pair formation; (3) existence of onset temperature T_{dyn} for dynamic superconductivity with phase fluctuations (dotted line), and (4) microscopic phase separation in the overdoped region, as illustrated in the inset figure.

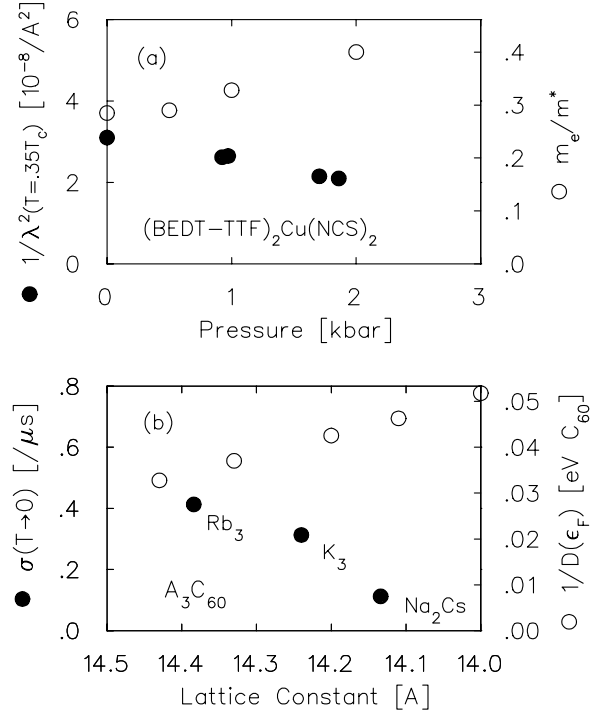


FIG. 18. Variation of the superfluid density (closed circle), obtained from the penetration depth as $1/\lambda^2$, and the corresponding normal state spectral weight n_n/m^* (open circles) in (a) organic 2-d superconductors $(\text{BEDT-TTF})_2\text{Cu}(\text{NCS})_2$ under applied pressure [62,63], and in (b) the alkali doped fulleride A_3C_{60} superconductors with varying size of alkali atoms A [17,18]. The behavior of n_n/m^* is inferred from that of $1/m^*$ in quantum oscillation studies [63] in (a), while the inverse of the density of states at the Fermi level [63] in A_3C_{60}